

# BET inhibitors synergize with venetoclax to induce apoptosis in MYC-driven lymphomas with high BCL-2 expression

Thomas E. C. Cummin,<sup>1</sup> Kerry L. Cox,<sup>1</sup> Tom D. Murray,<sup>1</sup> Anna H. Turaj,<sup>1</sup> Lisa Dunning,<sup>2</sup> Vikki L. English,<sup>2</sup> Rachel Fell,<sup>3</sup> Graham Packham,<sup>3</sup> Yan Ma,<sup>4</sup> Ben Powell,<sup>4</sup> Peter W. M. Johnson,<sup>3</sup> Mark S. Cragg,<sup>1</sup> and Matthew J. Carter<sup>1</sup>

<sup>1</sup>Antibody and Vaccine Group, Centre for Cancer Immunology, <sup>2</sup>Preclinical Unit, Centre for Cancer Immunology, and <sup>3</sup>Cancer Research UK Centre, Cancer Sciences Unit, Faculty of Medicine, University of Southampton, Southampton, United Kingdom; and <sup>4</sup>Plexikon Inc., Berkeley, CA

## Key Points

- Novel BET inhibitors PLX51107 and PLX2853 induce apoptosis via induction of the proapoptotic BH3-only protein BIM.
- PLX51107 and PLX2853 are synergistic with ABT199/venetoclax in killing MYC-driven B-cell lymphoma cells with high BCL-2 expression.

Although the MYC oncogenic network represents an attractive therapeutic target for lymphoma, MYC inhibitors have been difficult to develop. Alternatively, inhibitors of epigenetic/ transcriptional regulators, particularly the bromodomain and extraterminal (BET) family, have been used to modulate MYC. However, current benzodiazepine-derivative BET inhibitors (BETi) elicit disappointing responses and dose-limiting toxicity in relapsed/ refractory lymphoma, potentially because of enrichment of high-risk molecular features and chemical backbone-associated toxicities. Consequently, novel nonbenzodiazepine BETi and improved mechanistic understanding are required. Here we characterize the responses of aggressive MYC-driven lymphomas to 2 nonbenzodiazepine BETi: PLX51107 and PLX2853. Both invoked BIM-dependent apoptosis and in vivo therapy, associated with miR-17~92 repression, in murine E $\mu$ -myc lymphomas, with PLX2853 exhibiting enhanced potency. Accordingly, exogenous BCL-2 expression abrogated these effects. Because high BCL-2 expression is common in diffuse large B-cell lymphoma (DLBCL), BETi were ineffective in driving apoptosis and in vivo therapy of DLBCL cell lines, mirroring clinical results. However, BETi-mediated BIM upregulation and miR-17~92 repression remained intact. Consequently, coadministration of BETi and ABT199/venetoclax restored cell death and in vivo therapy. Collectively, these data identify BIM-dependent apoptosis as a critical mechanism of action for this class of BETi that, via coadministration of BH3 mimetics, can deliver effective tumor control in DLBCL.

## Introduction

Despite the effective rituximab, cyclophosphamide, doxorubicin, vincristine, prednisone (R-CHOP) treatment regimen, relapsed/refractory (R/R) disease is common in diffuse large B-cell lymphoma (DLBCL), with further intervention currently associated with poor tolerability and survival.<sup>1</sup> Consequently, additional treatment options are required.

Cell of origin (COO) classifiers identify 3 DLBCL subsets: activated B cell (ABC), germinal center B cell (GCB), and unclassified.<sup>1</sup> There is heterogeneity of prognosis within these, according to features associated with R-CHOP resistance, centered on MYC and BCL-2.<sup>2</sup> High coexpression without underlying chromosomal rearrangement defines the double expressor lymphoma (DEL) subgroup, most common within ABC-DLBCL, whereas, the largely GCB-DLBCL-associated double-hit lymphoma (DHL) represent high-grade lymphomas with MYC and BCL-2 or BCL-6 translocations.<sup>2</sup> Both DHL and DEL exhibit poor prognosis<sup>3</sup> and are over-represented in R/R cases (~50% DEL and 13% DHL).<sup>4</sup>

Submitted 4 May 2020; accepted 13 June 2020; published online 27 July 2020. DOI 10.1182/bloodadvances.2020002231.

Data may be requested from the corresponding author at m.j.carter@soton.ac.uk.

The full-text version of this article contains a data supplement.  
© 2020 by The American Society of Hematology



immunoprecipitation were undertaken using standard techniques, as previously described.<sup>25</sup> For immunoprecipitation experiments, lysis was undertaken using 3-[(3-cholamidopropyl)dimethylammonio]-1-propanesulfonate (CHAPS) lysis buffer (20 mM Tris pH 7.4, 142.5 mM KCl, 2 mM CaCl<sub>2</sub>, 1% CHAPS) with anti-human BCL-2 (clone: 6C8) and anti-mouse BCL-2 (clone: 3F11) (both BD Biosciences, Oxford, United Kingdom) used as the precipitating antibody vs an anti-human CD18 isotype control (HB226). Coimmunoprecipitated proteins were detected using Veriblot horseradish peroxidase-conjugated antibodies (Abcam, Cambridge, United Kingdom).

## Cellular assays and retroviral transduction

Annexin V/propidium iodide (PI) and DiOC6/ PI viability assays, hypotonic PI cell cycle assays, and BIM RNAi via retroviral transduction were performed as previously described.<sup>24-26</sup> For further details and other methods, see the supplemental Methods.

## Results

### PLX51107 and PLX2853 modulate BET biomarker expression

To investigate the therapeutic potential and mechanisms of action of PLX51107 and PLX2853, aggressive MYC-driven lymphoma models were used; namely, established human B-lymphoma cell lines (supplemental Tables 1 and 2) and spontaneous IgM<sup>+</sup> murine E $\mu$ -myc lymphoma cell lines (LCLs) derived from transgenic (Tg) animals.<sup>27</sup> PLX51107 exhibited a maximum plasma concentration of ~50  $\mu$ M 1 hour after treatment, falling to ~10  $\mu$ M after 8 hours after a single 20-mg/kg dose in mice.<sup>23</sup> To assess on-target activity, validated BET biomarker (*HEXIM1* and *MYC*) expression was assessed at physiologically relevant concentrations ( $\leq 10$   $\mu$ M).<sup>6,28</sup> Both PLX51107 and PLX2853 increased *HEXIM1* mRNA and decreased *MYC* mRNA and protein expression in human LCLs (supplemental Figure 1A-C). PLX2853 exhibited enhanced potency, with increases in *HEXIM1* detectable at lower concentrations. Similar increases in *HEXIM1* transcript and reduction of *MYC* protein expression were also observed in E $\mu$ -myc LCLs (supplemental Figure 1D-E). These observations indicate effective BET inhibition in both human and murine lymphoma models.

### PLX51107 and PLX2853 elicit intrinsic apoptosis in E $\mu$ -myc lymphoma cell lines

Administration of benzodiazepine-derivative BETi (JQ1 and OTX015) has been associated with cell death.<sup>15,29</sup> Consistent with these effects, PLX51107 and PLX2853 reduced viability (staining exemplified in supplemental Figure 2A) in E $\mu$ -myc LCLs, with PLX2853 exhibiting greater potency than PLX51107 and benzodiazepine-derivative BETi (Figure 1A-B). PLX51107- and PLX2853-induced cell death displayed hallmarks of apoptosis,<sup>30</sup> as death was abrogated by the pan-caspase inhibitor qVD (Figure 1C). To further dissect their BETi-induced apoptosis, E $\mu$ -myc LCLs were engineered to overexpress (OE) negative regulators of intrinsic apoptosis, BCL-2, or BCL-XL (supplemental Figure 3A-B). Crucially, these engineered cell lines retained BETi-mediated increases in *HEXIM1* mRNA and reduction in *MYC* protein levels (supplemental Figure 3C-D).

Analogous to qVD, BCL-2 or BCL-XL OE abrogated PLX51107- and PLX2853-induced cytotoxicity (Figure 1D). These data indicate that PLX51107 and PLX2853 invoke cell death via intrinsic or type II extrinsic apoptosis. To scrutinize this, BETi-induced change in mitochondrial membrane potential ( $\Delta\psi_m$ ), indicative of MOMP, was examined (supplemental Figure 2B). PLX51107 and PLX2853 invoked substantial  $\Delta\psi_m$  that was ameliorated by BCL-2 or BCL-XL OE but not by qVD (Figure 1E). Consequently, intrinsic apoptosis (requiring prior caspase-independent MOMP and downstream caspase activation) represents their mechanism of cell killing. Consistent with this, both PLX51107 and PLX2853 showed significant *in vivo* therapeutic responses in wild-type, but not BCL-2 OE, E $\mu$ -myc lymphoma-bearing mice (Figure 1F). Thus, similarly to benzodiazepine-derivative BETi,<sup>15</sup> intrinsic apoptosis was identified as the therapeutic mechanism for PLX51107 and PLX2853 in E $\mu$ -myc lymphomas.

### PLX51107 and PLX2853 upregulate the BH3-only protein BIM in E $\mu$ -myc lymphoma cell lines

To identify key molecular regulators of nonbenzodiazepine BETi-induced apoptosis, BCL-2 family member expression was examined after PLX51107 or PLX2853 application. Increased expression of the proapoptotic BH3-only protein BIM was observed at both mRNA and protein levels in wild-type E $\mu$ -myc LCLs (Figure 2A-C), with PLX2853-induced increases evident at lower concentrations in 3 of 3 cell lines. Increased BIM protein expression was also observed in BCL-2 OE E $\mu$ -myc LCLs (Figure 2D, left; supplemental Figure 2C). Both agents increased association between BIM and BCL-2, representing enhanced mitochondrial priming, in both BCL-2 OE and wild-type E $\mu$ -myc LCLs (Figure 2D-E; supplemental Figure 2D). *PUMA* and *BMF* transcripts were also elevated in response to BETi; however, these were not reflected at the protein level (supplemental Figure 4A-B). *BCL-2/BCL-XL* expression appeared only minimally affected by BETi, although reduced *BCL-XL* was apparent in 1 cell line. In contrast, both *MCL-1* and *BCL-2A1* transcripts were significantly upregulated (supplemental Figure 4A). Previously, BCL-2A1/BFL-1 was identified as a critical driver of ABT-199/venetoclax resistance in DLBCL cell lines that was downregulated by benzodiazepine-derivative BETi.<sup>31</sup> However, MCL-1 protein remained unaffected by nonbenzodiazepine BETi, and BCL-2A1 was undetectable (supplemental Figure 4B).

### PLX51107 and PLX2853 invoke BIM-dependent apoptosis in E $\mu$ -myc lymphoma cell lines

To test the relevance of impaired MYC target transactivation after BETi and BRD4 loading of its promoter,<sup>15</sup> the effect of PLX51107 and PLX2853 on the miR-17~92 miRNA cluster was assessed. miR-17~92 represents a key target of MYC, required for repression of tumor suppressors (including BIM) to elicit the oncogenic program.<sup>32</sup> Both PLX51107 and PLX2853 robustly downregulated the BIM targeting<sup>33-36</sup> miRNAs miR-17-5p and -92a (Figure 3A). Overall, a trend toward reduced expression was evident across the miR-17~92 locus, although because of cell line variation, this was not statistically significant in most cases (supplemental Figure 4C). To determine the contribution of BIM toward PLX51107- and PLX2853-induced apoptosis, BIM-targeted RNAi and BIM<sup>-/-</sup> (KO) E $\mu$ -myc LCLs were used.

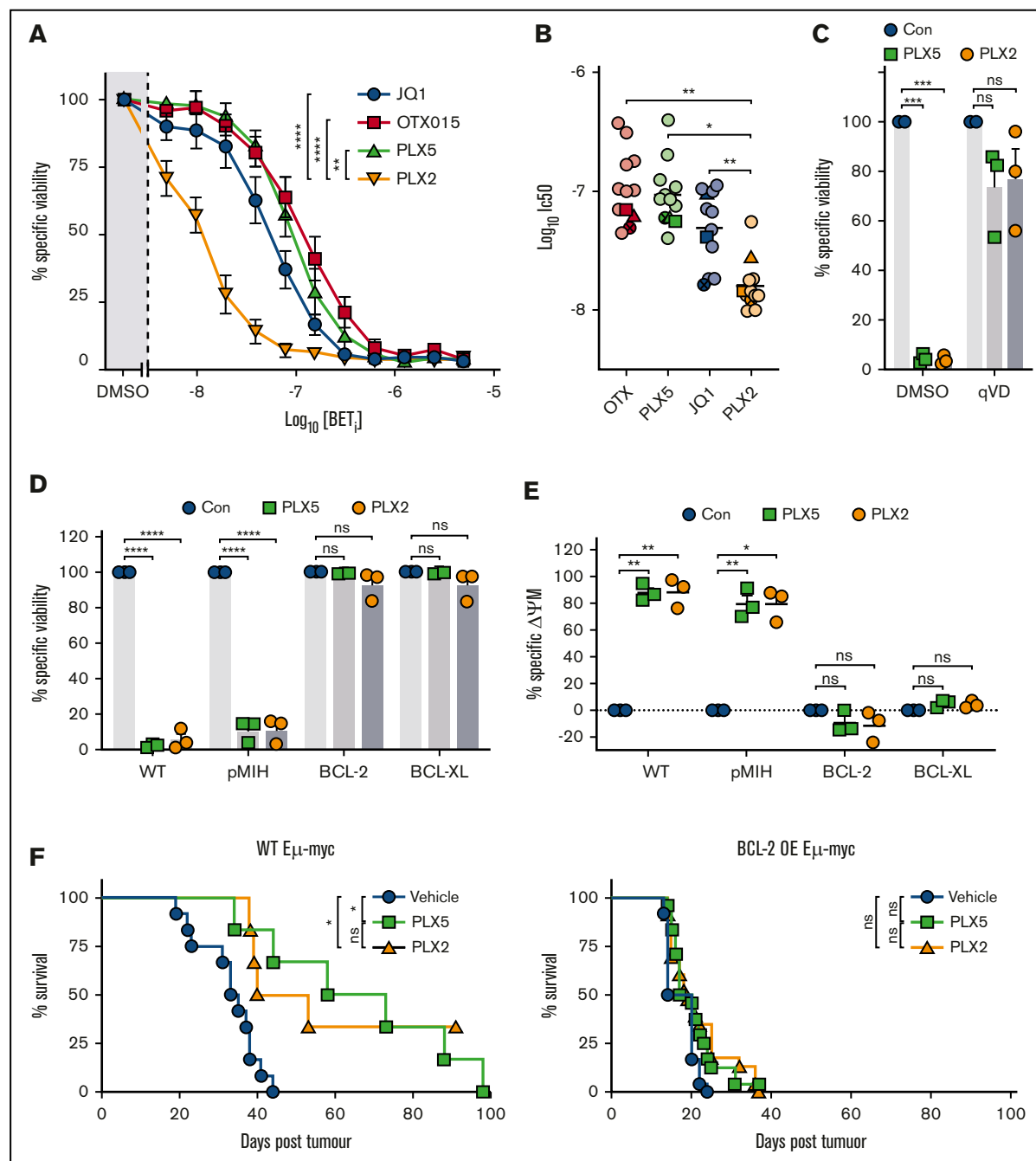


**Figure 1. PLX51107 and PLX2853 BETi invoke cell death via intrinsic apoptosis in Eμ-myc lymphomas.** (A) PLX51107 (PLX5), PLX2853 (PLX2), JQ1, and OTX015 were administered to Eμ-myc lymphoma cell lines for 48 hours, and viability was assessed by annexin V/PI staining vs vehicle control (dimethyl sulfoxide [DMSO]). Points represent the mean of 12 wild-type (WT) cell lines, each performed in triplicate, normalized to control viability and expressed as percentage specific viability. (B) Data from panel A were used to calculate IC<sub>50</sub>s. Darker shaded symbols represent cell lines used for subsequent in vitro experimentation. Crossed circles denote the AH29 lymphoma cell line, triangles denote AF47, and squares denote Eμ# 4. (C) Eμ-myc lymphoma cell lines (n = 3), pretreated with 25 μM qVD or a DMSO vehicle control for 1 hour, were exposed to 1000 nM PLX5, 100 nM PLX2, or an additional vehicle control (Con) and viability assessed as in panel A. (D-E) WT, control (pMIH), or BCL-2/BCL-XL transduced Eμ-myc lymphoma cell lines treated with 1000 nM PLX5, 100 nM PLX2, or a DMSO vehicle control (Con) were assessed for viability (D) and changes in mitochondrial membrane potential (ΔΨ<sub>m</sub>) (E) by annexin V/PI or DiOC<sub>6</sub>/PI staining, respectively. Points in panels C-E represent the mean of 3 independent experiments for each cell line, performed in triplicate. (F) Matched WT or BCL-2-transduced Eμ-myc lymphoma-bearing C57BL/6 were treated with (n = 7) 10 mg/kg PLX5, (n = 6) 5 mg/kg PLX2, or (n = 11) vehicle control, starting 4 days after engraftment and survival was assessed. Data are collated from 2 independent experiments using 2 different matched pairs of WT and BCL-2-transduced Eμ-myc lymphoma cell lines. Error bars represent standard error of the mean (SEM). Statistical analyses were performed using 1-way (B) or 2-way analysis of variance (ANOVA) (A and C-E) and P values adjusted using Tukey's or Dunnett's multiple comparisons tests. In panel A, asterisks represent comparisons of overall curves between different conditions. Survival analysis was performed using a log-rank test adjusted for multiple comparisons using the Holm-Sidak method. \*\*\*\*P < .00005, \*\*\*P < .0005, \*\*P < .005, \*P < .05. ns, nonsignificant.



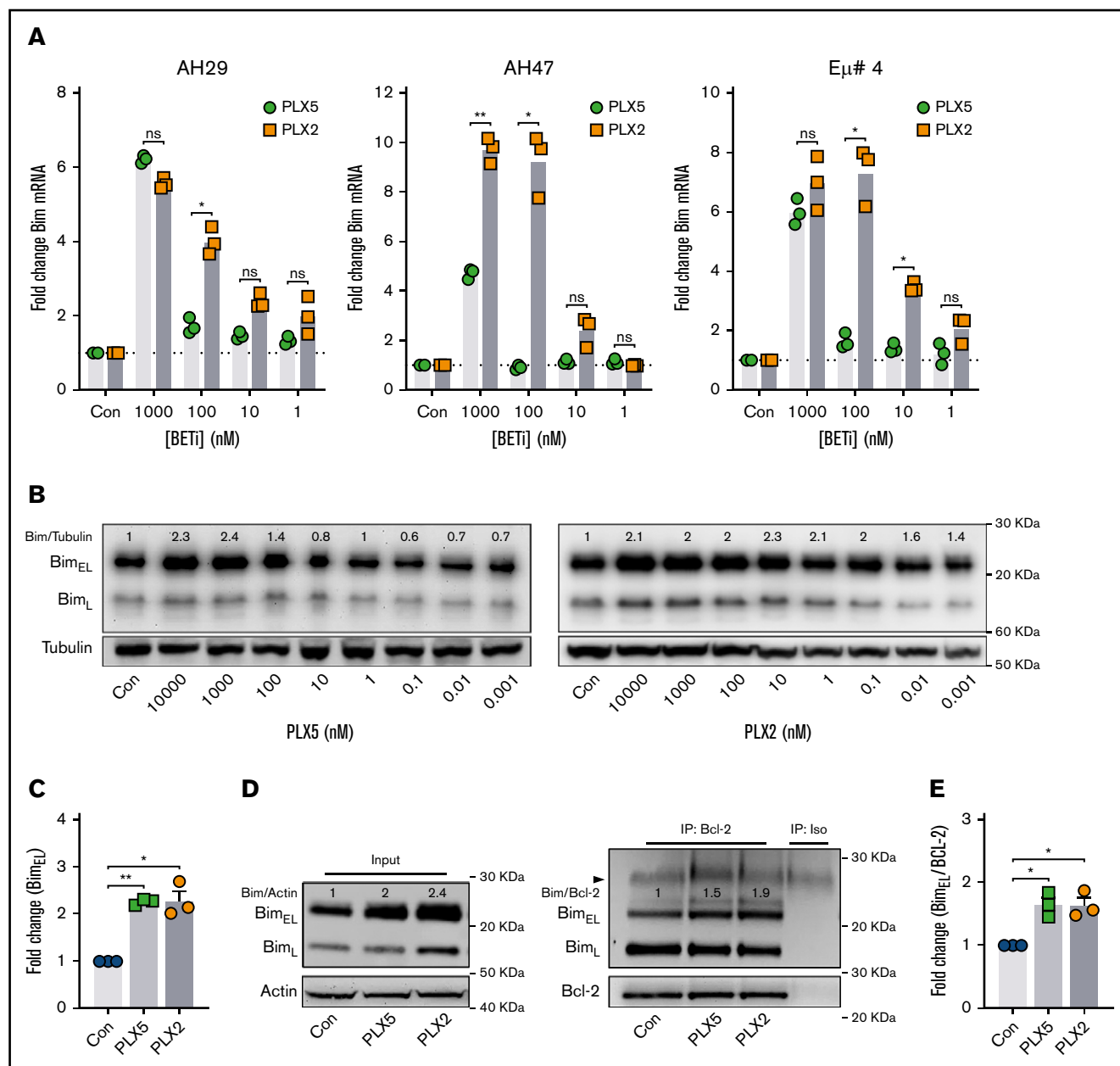


**Figure 2. PLX51107 and PLX2853 BETi upregulate the BH3-only protein BIM in Eμ-myc lymphomas.** (A) Eμ-myc lymphoma cell lines (AH29, AH47, and Eμ# 4) were treated with qVD (25 μM) for 1 hour to inhibit cell death, followed by PLX5, PLX2, or a DMSO vehicle control (Con) for 24 hours. *BIM* mRNA expression was then assessed, in triplicate, by quantitative polymerase chain reaction (qPCR) normalized to GAPDH. (B) Eμ-myc lymphoma cell lines (n = 3) were treated as in panel A, and BIM protein expression was assessed after 48 hours. (B) Representative example, with densitometry data normalized to a DMSO control (Con) for 1000 nM PLX5 or PLX2 from each cell line depicted in panel C. (D-E) BCL-2 OE Eμ-myc lymphoma cell lines (n = 3) were treated with 1000 nM PLX5 or PLX2 or a DMSO vehicle control (Con), and BCL-2 protein was immunoprecipitated after 48 hours. Levels of BIM coimmunoprecipitation were then assessed. (D) Representative example of input whole cell lysates (i) and BIM:BCL-2 coimmunoprecipitation (ii) with coimmunoprecipitation densitometry data normalized to baseline demonstrated in panel E. Error bars represent SEM. Statistical analysis was performed using 2-way (A) or 1-way (C-E) ANOVA, and *P* values were adjusted using the Sidak method or Dunnett's multiple comparisons tests, respectively. \*\**P* < .005, \**P* < .05.

BIM shRNA generated ~75% knockdown (KD) of expression (supplemental Figure 4D). PLX51107- and PLX2853-induced apoptosis appeared unaffected by control transduction (supplemental Figure 4E) but was substantially reduced after BIM KD (Figure 3B). As confirmation, BIM<sup>-/-</sup> Eμ-myc LCLs, derived from Bim<sup>-/-</sup> Eμ-myc Tg mice,<sup>37</sup> were assessed and an analogous

reduction in BETi-induced cell death observed (supplemental Figure 4F). Despite this, BIM KO/KD failed to fully ablate PLX51107- and PLX2853-induced apoptosis, unlike exogenous BCL-2 or BCL-XL expression (Figures 1D and 3B; supplemental Figure 5). Consequently, additional proapoptotic BCL-2 family members are likely to exert an effect. Despite this, Eμ-myc LCLs

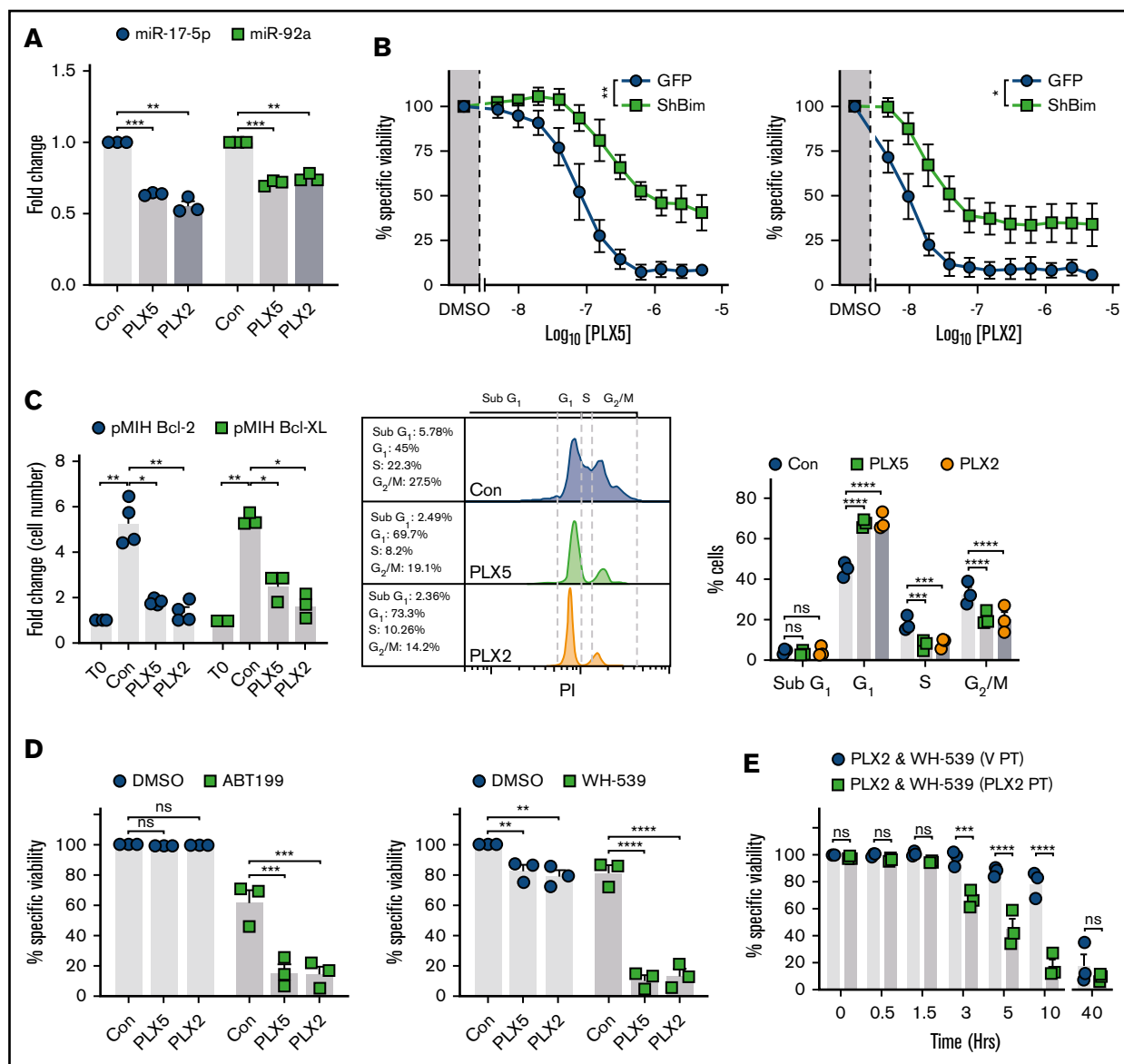


**Figure 3. PLX51107 and PLX2853 BETi-induced apoptosis is BIM dependent and effectively combines with BH3-mimetics in Eμ-myc lymphomas.**

(A) Eμ-myc lymphoma cell lines (n = 3) were treated as in Figure 2A and subjected to 1000 nM PLX5, 100 nM PLX2, or vehicle control (Con) for 24 hours. miR-17-5p and -92a expression was then assessed in triplicate by qPCR normalized to U6 snRNA. (B) Empty vector (GFP) or shBIM-transduced Eμ-myc lymphoma cell lines (n = 3) were treated with PLX5 or PLX2 and assessed for viability as in Figure 1A. Data represent the average of 3 independent experiments for each cell line, performed in triplicate. (C) Proliferation of BCL-2- (n = 4) or BCL-XL-transduced (n = 3) Eμ-myc lymphoma cell lines treated with 1000 nM PLX5, 100 nM PLX2, or a DMSO vehicle control (Con) were assessed after 48 hours and depicted as fold change in cell count compared with time 0 (T0). (Cii-iii) BCL-2-transduced (n = 3) Eμ-myc lymphoma cell lines were treated as in panel i and subjected to cell cycle analysis by hypotonic PI staining. (ii) Representative example of hypotonic PI staining. (iii) Representative example of hypotonic PI staining. (D) BCL-2- (i) or BCL-XL-OE (ii) Eμ-myc lymphoma cell lines were treated with 1000 nM PLX5, 100 nM PLX2, or an appropriate vehicle control (Con) alongside 300 nM ABT199 (i), 10 μM WEHI-539 (WH-539) (ii), or an additional vehicle control (DMSO) for 48 hours, and viability was assessed by annexin V/PI staining. Points represent the average of 3 independent experiments, performed in triplicate, for each cell line. (E) BCL-XL-transduced Eμ-myc lymphoma cell lines (n = 3) were pretreated with 100 nM PLX2 (PLX2 PT) or a vehicle control (V PT) for 24 hours before administration of 10 μM WEHI-539 (WH-539) and 100 nM PLX2, and viability was assessed after 48 hours. Final PLX2 concentration was 100 nM in all cases. Each point represents the average of triplicate data for each cell line. Statistical analyses were performed via 2-way ANOVA. P values were adjusted for multiple comparisons using either Dunnett's or Sidak's analyses, where appropriate, according to experimental design. \*\*\*\*P < .00005, \*\*\*P < .0005, \*\*P < .005, \*P < .05. Asterisks in panel B represent overall comparisons between curves. Error bars represent SEM.

derived from PUMA<sup>-/-</sup>, BMF<sup>-/-</sup>, NOXA<sup>-/-</sup>, or BIK<sup>-/-</sup> animals generated in Happon et al.<sup>38</sup> and Michalak et al.<sup>39</sup> exhibited analogous PLX51107- or PLX2853-induced apoptosis to their wild-type

counterparts, indicating that a more complex mechanism may generate additional cytotoxicity (supplemental Figure 5). Collectively, these observations identify BIM as a major driver of BETi-induced apoptosis.

## BH3 mimetics resensitize BCL-2 or BCL-XL high Eμ-myc lymphoma cell lines to BETi-induced cell death

These data imply that BETi monotherapy is unlikely to be effective in the treatment of B-cell malignancies with high prosurvival BCL-2 family member expression (eg, DEL and most DHL DLBCL) because of their enhanced capacity to neutralize BIM. To identify potential sensitization strategies, BCL-2 or BCL-XL OE Eμ-myc LCLs were used to model these treatment resistant malignancies. Despite lacking apoptotic and therapeutic responses, BCL-2 or BCL-XL OE Eμ-myc LCLs exhibited reduced proliferation, G1 cell cycle arrest, reduced S- and G2/M-phase entry, and elevated BIM expression in response to BETi (Figures 3C and 2D; supplemental Figure 2C). Because both PLX51107 and PLX2853 evoke enhanced BIM-mediated mitochondrial priming (Figure 2D-E; supplemental Figure 2D), we reasoned that coapplication of an appropriate BH3 mimetic (ABT199 for BCL-2 OE, WEHI-539<sup>40</sup> for BCL-XL OE) would provoke potent cell death. As expected, exogenous BCL-2 expression sensitized cells to the BCL-2-selective BH3 mimetic ABT199 because of stabilization of BIM expression and increased BIM:BCL-2 association<sup>41,42</sup>; however, this was not reflected by BCL-XL OE after WEHI-539-mediated BCL-XL inhibition (supplemental Figure 3E-F). Accordingly, coadministration of BH3 mimetics alongside a BETi effectively resensitized BCL-2/BCL-XL OE cells to BETi-induced cell death (Figure 3D). Because this combination effect likely requires BETi-mediated BIM upregulation to propagate the effect of BH3 mimetics, prior BETi application may accelerate cell death on BH3 mimetic exposure. An additional 24-hour PLX2853 pretreatment (72 hours total) did not enhance BETi-induced cytotoxicity in comparison with vehicle pretreatment (24 hours of vehicle followed by 48 hours of PLX2853; supplemental Figure 6A-B). However, a more rapid induction of cell death was indeed observed on BH3 mimetic application in comparison with simultaneous compound administration, with responses converging after 48 hours. This was apparent for WEHI-539 (Figure 3E) and, to a lesser extent, ABT199-containing combinations (supplemental Figure 6C). Consequently, appropriate BETi:BH3 mimetic combinations may represent an effective therapeutic approach for MYC-driven BCL-2-high malignancies, such as DEL and most DHL DLBCL.

## BETi:BH3 mimetic combinations are synergistic in MYC- and BCL-2-activated DLBCL cell lines

To explore the use of nonbenzodiazepine BETi:BH3 mimetic combinations in human cells, we performed similar experiments in human MYC- and BCL-2-activated GCB DLBCL cell lines (supplemental Table 1). Their relative BIM, BCL-2, and MYC expression profiles are exemplified in supplemental Figure 7A. As expected, MYC- and BCL-2-activated DLBCL cell lines were resistant to BETi-induced cell death (Figure 4A), likely attributable to the increased BIM neutralization capacity afforded by high BCL-2 expression. Consistent with this, PLX51107 and PLX2853 increased BIM protein expression and BCL-2 association (mitochondrial priming) in all cell lines analyzed (Figure 4B-C; supplemental Figure 7B-D). Consequently, resistance to BETi-mediated apoptosis is not attributable to lack of BIM upregulation. Furthermore, human Burkitt lymphoma-derived cell lines, which commonly carry

MYC but not BCL-2 translocations, consistently demonstrated elevated BIM protein after PLX51107 or PLX2853 treatment (supplemental Figure 8). BETi-induced BIM upregulation correlated with suppression of miR-17-5p and -92a (Figure 4D) with a variable nonstatistically significant trend toward reduction of other miR-17~92 constituents (supplemental Figure 7E). Collectively, these data reflect our findings in murine B-lymphoma models. Correspondingly, BETi:ABT199 combinations were synergistic in MYC- and BCL-2-activated DLBCL cell lines, as reported previously for benzodiazepine-derivative BETi<sup>31,43,44</sup> (Figure 5A-B; supplemental Figure 9A-B). Consequently, high BCL-2 expression represents a key mediator of BETi-resistance in these cells.

To determine the role of BIM in this combination and delineate the mechanism of BCL-2-mediated BETi resistance, SUDHL6 cells were subjected to BIM-targeted RNAi with ~44% BIM KD achieved (Figure 5C, left). Control transduction did not influence BETi-, ABT199-, or combination-induced cytotoxicity. However, BIM KD effectively ablated the combination effect of BETi:ABT199 (Figure 5C, right), indicating a dependence on BIM in these cells. Furthermore, these observations identify that high BCL-2 expression drives resistance to BETi-induced apoptosis via neutralization of BETi-upregulated BIM. As a proof of concept, primary human lymphoma cells were subjected to nonbenzodiazepine BETi:BH3 mimetic combination therapy. Primary lymphomas exhibited higher cell death in response to PLX2853:ABT199 combinations compared with either agent alone (supplemental Figure 9C).

## BETi:BH3 mimetic combinations demonstrate effective tumor control in MYC- and BCL-2-activated DLBCL xenografts

To determine the in vivo efficacy of BETi:ABT199 combination therapy, the MYC- and BCL-2-translocated DHL DLBCL cell lines SUDHL6 and OCI-LY8 were engrafted into NSG animals. PLX2853, ABT199, and combinations thereof appeared tolerable with no measurable changes in body weight attributable to treatment (supplemental Figure 10). In these models, PLX2853 monotherapy failed to elicit therapeutic responses at doses effective in wild-type Eμ-myc lymphoma-bearing animals, potentially attributable to BCL-2-mediated neutralization of BETi-upregulated BIM, as predicted from in vitro data. Likewise, ABT199 monotherapy was ineffective in these models, presumably because of suboptimal mitochondrial priming in the absence of further apoptotic stimuli. Accordingly, coadministration of ABT199 alongside BETi circumvented the BCL-2-mediated block in intrinsic apoptosis, effectively resensitizing cells to BETi, resulting in a rapid and durable reduction in tumor volume and increased overall survival (Figure 6A-C).

Collectively, our data demonstrate that nonbenzodiazepine BETi PLX51107 and PLX2853 upregulate the key BH3-only protein BIM, coincident with suppression of BIM-targeting miRNAs, to deliver potent cytotoxic responses and in vivo therapy in BCL-2-low MYC-driven tumors. In contrast, BCL-2-high tumors escape this fate via their increased capacity to bind and neutralize BIM. This mechanistic knowledge can be leveraged to deliver effective in vivo therapy for BCL-2-high MYC-driven tumors via coadministration of an appropriate BH3 mimetic, to deliver durable in vivo tumor control. As such, alteration of the underlying chemical structure of BETi does not alter their therapeutic mechanism.<sup>15,29</sup>

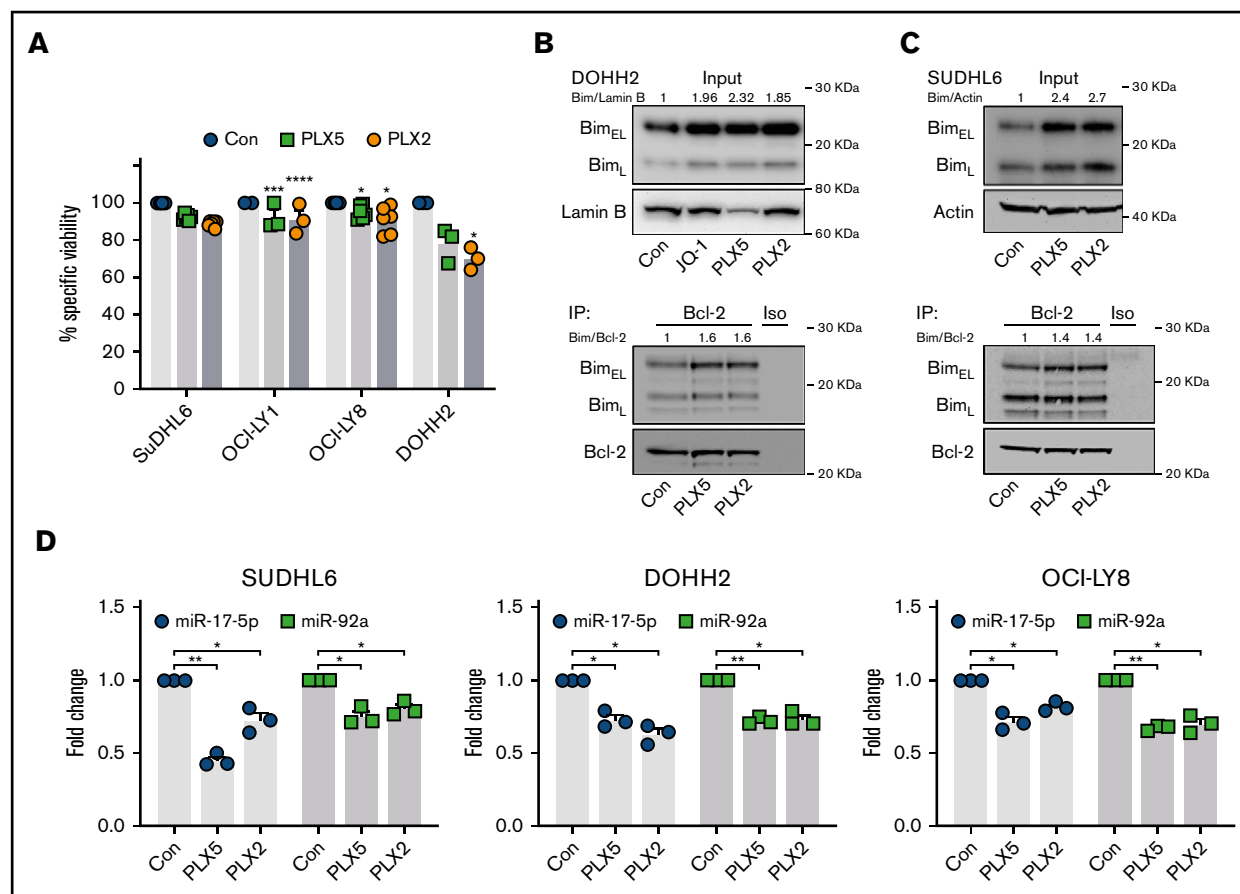


**Figure 4.** PLX51107 and PLX2853 BETi upregulate BIM in DHL/DEL DLBCL cell lines. (A) SUDHL6, OCI-LY1, OCI-LY8, and DOHH2 were treated with 1000 nM PLX5, 100 nM PLX2, or a DMSO vehicle control (Con) for 48 hours, and viability was assessed by annexin V/PI staining. Points depict the averages of 3 to 6 independent experiments per cell line, each performed in triplicate. (B-C) DOHH2 or SUDHL6 were treated as in panel A, and BIM protein expression was assessed (i). Lysates were subjected to BCL-2 immunoprecipitation and assessed for BIM coimmunoprecipitation (ii). (D) SUDHL6, DOHH2, and OCI-LY8 were treated with 1000 nM PLX5, 100 nM PLX2, or DMSO vehicle control (Con) for 24 hours, and miR-17-5p and -92a expression was assessed by qPCR in triplicate. U6 snRNA was used as an internal control. Error bars represent SEM. Statistical analyses were performed by 2-way ANOVA, and *P* values were adjusted using Dunnett's multiple comparisons tests. \*\*\*\**P* < .00005, \*\*\**P* < .0005, \*\**P* < .005, \**P* < .05.

However, the greater potency of PLX2853 and the potential for reduced toxicity offered by nonbenzodiazepine BETi may allow the clinical potential of BETi to be realized.

## Discussion

Because of their ability to modulate the MYC oncogenic network and induce cytotoxicity, BETi represent promising therapeutic agents for B-cell lymphoma.<sup>6,11</sup> Despite this, modest responses at the edge of tolerability have limited clinical application of benzodiazepine-derivative BETi in R/R B-lymphoma.<sup>18-20</sup>

Here we characterized the activities of 2 novel nonbenzodiazepine BETi, PLX51107<sup>23</sup> and PLX2853, in murine and human models of MYC-driven lymphoma. PLX51107 and PLX2853 modulated BET biomarker expression (MYC and *HEXIM1*), consistent with on-target inhibition,<sup>6,28</sup> and exhibited potent cytotoxicity in the nanomolar range in Eμ-myc LCLs. Consistent with benzodiazepine-derivative BETi,<sup>15,29</sup> PLX51107 and PLX2853 upregulated the key BH3-only protein BIM, coincident with repression of miR-17~92 cluster constituents miR-17-5p

and -92a, leading to BIM-dependent intrinsic apoptosis and in vivo therapeutic responses. In particular, PLX2853 demonstrated elevated potency in comparison with PLX51107 (and benzodiazepine-derivative BETi) in numerous experimental readouts.

BIM represents a critical apoptotic driver during cytotoxic cellular insult, oncogenesis, and development and is central to B-cell homeostasis.<sup>37,45,46</sup> This activity is manifest in deletion of mature B cells following disruption of tonic B-cell receptor (BCR) signaling,<sup>25</sup> removal of autoreactive B cells,<sup>47</sup> and suppression of MYC-driven lymphomagenesis.<sup>37</sup> In this latter role, BIM appears to be a direct transcriptional target of MYC.<sup>45</sup> However, these activities are repressed by the miR-17~92 cluster (itself a MYC target).<sup>32</sup> In a direct phenocopy of BIM<sup>-/-</sup> mice,<sup>46</sup> forced miR-17~92 expression drives autoimmunity through BIM suppression, via direct binding of miR-17-5p and -92 to the BIM 3' untranslated region.<sup>33-36</sup> Furthermore, miR-17~92 KO imparts B-cell deletion associated with elevated BIM expression.<sup>35</sup> Consequently, the BIM: miR-17~92 axis represents a key regulator of B-cell development.



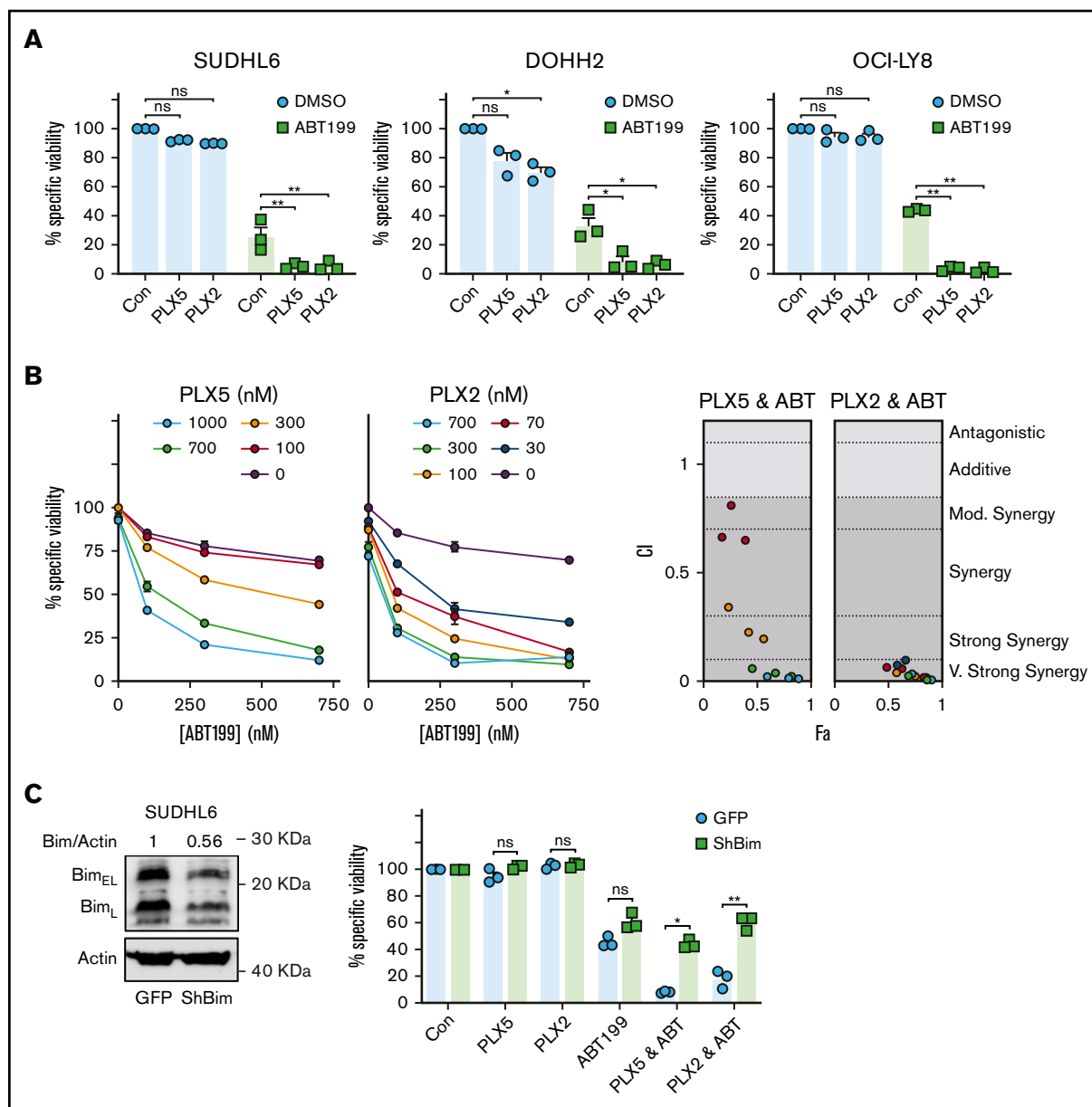


**Figure 5. PLX51107 and PLX2853 BETi effectively combine with ABT199 in DHL/DEL cell lines.** (A) SUDHL6, DOHH2, and OCI-LY-8 were treated with 1000 nM PLX5, 100 nM PLX2, or a vehicle control (Con) alongside 600 nM ABT199 or an additional vehicle control (DMSO) for 48 hours, and viability was assessed by annexin V/PI staining. (Bi) SUDHL6 was subjected to a dose titration of PLX5 or PLX2 in the presence of increasing ABT199 concentrations and assessed for viability after 48 hours by annexin V/PI staining. Doses (0 nM) represent the addition of an appropriate DMSO vehicle control. (Bii) SUDHL6 data were assessed for synergy using the Chou-Talalay method and CompuSyn software. Points are color coded according to PLX5/PLX2 dose depicted in panel i. Data represent the average of triplicate data. (C) SUDHL6 were transduced with empty vector (GFP) or shBIM constructs, and BIM protein expression was assessed by western blotting (i). The impact of BIM knockdown on the combination of BETi and ABT199 was then assessed by treating SUDHL6 GFP/shBIM as described in panel A. Error bars represent SEM. Statistical analyses were performed using 2-way ANOVA and Dunnett's multiple comparison tests. \*\* $P < .005$ , \* $P < .05$ . Fa, effect; CI, combination index.

However, during MYC-driven oncogenesis, miR-17~92 facilitates and maintains the MYC-driven neoplastic state through suppression of BIM and epigenetic modifiers.<sup>32</sup> These effects appear reversed on experimental MYC inactivation, leading to BIM upregulation- and miR-17~92 repression-mediated tumor regression.<sup>32</sup> This antagonistic relationship appears subverted by the MYC oncogenic program and represents a prime therapeutic target. miR-17~92 genomic dysregulation is prevalent in GCB

DLBCL<sup>48</sup> and, where no genomic aberration is apparent, appears driven by upregulation of MYC activity independent of genetics.<sup>49</sup> Thus, BIM and miR-17~92 appear linked to the etiology of MYC-driven tumors.

Benzodiazepine-derivative BETi has been associated with BIM upregulation, ascribed to BETi-mediated removal of BRD4 from the miR-17~92 promoter.<sup>15,29</sup> Here, we expand on these findings and show equivalent effects for the novel nonbenzodiazepine BETi's

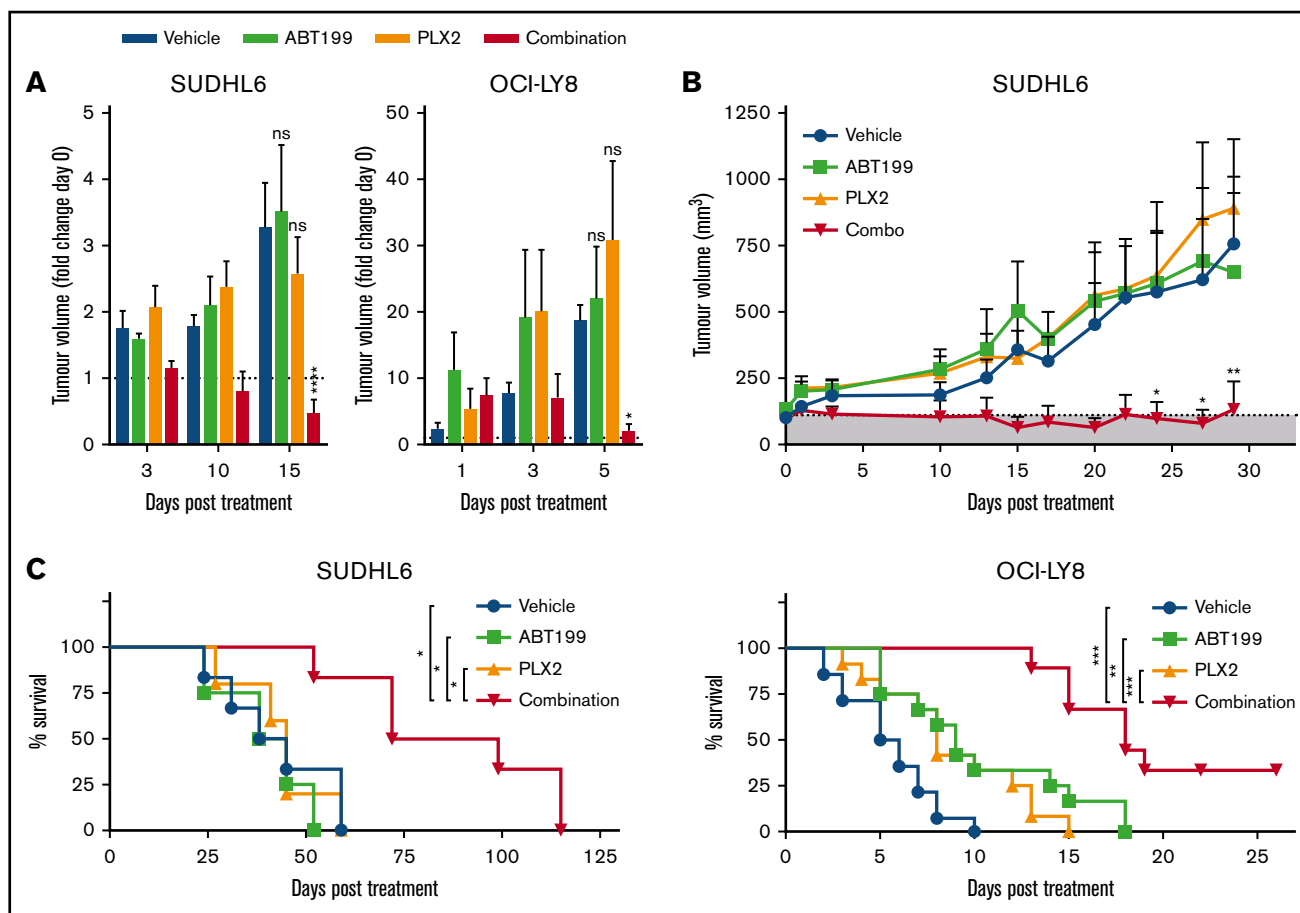


**Figure 6. PLX2853 BETi: ABT199 combination therapy enhances survival in DHL xenografts.** After detection of tumor growth, SUDHL6- or OCI-LY8-bearing NSG animals were randomized into treatment arms with equivalent mean tumor volume. Subsequently, animals were treated with 5 mg/kg PLX2853 (orally once daily), 50 mg/kg ABT199 (orally once daily), or both in combination, and tumor growth was monitored in comparison with a vehicle control (A-B). Animals were maintained on therapy until the humane end point was reached (OCI-LY8) or for 28 days (SUDHL6), and overall survival was assessed (C). Shaded area in panel B represents tumor size before start of treatment. OCI-LY8 data represent 2 independent experiments combined: vehicle (n = 14), ABT199 (n = 12), PLX2853 (n = 12), combination (n = 9). SUDHL6 data: vehicle (n = 6), ABT199 (n = 4), PLX2853 (n = 5), combination (n = 6). (A-B) Statistical analyses were performed using 2-way ANOVA and Dunnett's multiple comparisons test. (C) Survival analysis was performed using a log-rank test and Holm-Sidak multiple comparisons correction. Error bars represent SEM. \*\*\*\*P < .00005, \*\*\*P < .0005, \*\*P < .005, \*P > .05.

PLX51107 and PLX2853. Consequently, our and others' data demonstrate a direct requirement for BIM induction in BETi-induced apoptosis and in vivo therapy,<sup>15</sup> independent of underlying chemical structure. In contrast to experimental MYC inactivation,<sup>32</sup> the direct requirement for BETi-mediated MYC downregulation to drive BIM induction has been disputed.<sup>15,16</sup> This disparity may arise from enrichment of BRD4 at sites proximal to both MYC and miR-17~92 promoters.<sup>10,50</sup> Consequently, after BETi, both MYC and miR-17~92 may be independently repressed via displacement of BRD4.

Despite BIM KD or KO affording resistance toward BET-induced apoptosis, protection was not equivalent to that provided by BCL-2 or BCL-XL OE, which fully ablated intrinsic apoptosis (as described previously).<sup>15,29</sup> It is likely that additional BH3-only proteins may contribute. *BMF* and *PUMA* mRNA were upregulated after BETi. Both BMF and PUMA are implicated in apoptotic tumor suppression after oncogenic MYC dysregulation.<sup>39,51</sup> However, neither was robustly upregulated at the protein level, and KO of either gene

failed to offer protection to BETi. Potentially, a composite effect resulting from multiple small changes in other BH3-only proteins and/or prosurvival members in different tumors is responsible.

Because exogenous BCL-2 or BCL-XL abrogated cytotoxicity and therapeutic responses in Eμ-myc lymphomas, as described for benzodiazepine-derivative BETi,<sup>15,29</sup> PLX51107 or PLX2853 are unlikely to be effective in the treatment of BCL-2-high malignancies,<sup>15</sup> such as DEL and most DHL DLBCL.<sup>2</sup> Consequently, this may partly explain the disappointing clinical responses seen with benzodiazepine-derivative BETi to date.<sup>18</sup> Accordingly, BETi monotherapy was largely ineffective in driving cytotoxic responses and tumor control in MYC- and BCL-2-activated DLBCL cell lines/ primary lymphomas and DLBCL xenografts, respectively. Despite this, BETi-mediated repression of miR-17-5p/-92a and BIM upregulation remained intact. Consequently, neutralization of high BCL-2 expression, via use of the BCL-2-selective BH3 mimetic ABT199/venetoclax, effectively resensitized MYC- and BCL-2-activated DLBCL cell lines and primary lymphomas to

BETi-induced cell death and delivered durable antitumor responses in MYC- and BCL-2–translocated DLBCL xenografts. In line with our and others' data,<sup>15,29</sup> this combination effect was BIM dependent. Consequently, enhanced BETi-mediated mitochondrial priming (ie, elevated BIM:BCL-2 association) and subsequent ABT199/venetoclax-enabled displacement likely explains this synergistic effect, as suggested previously for other agents.<sup>25,52</sup> BETi:BH3 mimetic combinations may demonstrate particular efficacy in DLBCL, as proposed previously,<sup>31</sup> where high BCL-2 expression is common and associated with poor disease-free survival.<sup>3</sup>

Overall, these findings reflect data obtained using benzodiazepine-derivative BETi both alone and in combination with BH3 mimetics.<sup>15,31,53</sup> Consequently, differences in chemical class do not appear to alter the mechanisms of BETi. However, because current benzodiazepine-derivative BETi demonstrate limited clinical responses only at high poorly tolerated doses, the exquisite potency of PLX2853 and the lack of a benzodiazepine backbone (which itself may drive dose-limiting toxicity) may be important for clinical application,<sup>18</sup> providing the impetus for further development of PLX2853.

Because our MYC- and BCL-2–activated DLBCL cell lines were exclusively GCB, according to COO classification, the role of BETi-induced BIM upregulation in ABC-DLBCL remains unclear. ABC- and GCB-DLBCL exhibit substantial biological divergence; in particular, reliance on chronic BCR signaling and NF- $\kappa$ B oncogenic addiction in ABC-DLBCL.<sup>54</sup> Given the ability of BCR-dependent pathways to regulate BIM expression<sup>25</sup> and observations of chronic BCR-signaling in ABC-DLBCL,<sup>54</sup> mechanistic differences between COO subtypes may be apparent. Accordingly, NF- $\kappa$ B pathway inhibition has been observed after BETi in ABC DLBCL.<sup>55</sup> Presumably, BETi disrupt the BRD4:NF- $\kappa$ B p65 (RELA) interaction, preventing target gene transactivation and formation of new SEs on which ABC-DLBCL rely.<sup>54,56</sup>

Taken together, our data demonstrate that novel nonbenzodiazepine BETi's, PLX51107 and PLX2853, potentially upregulate the proapoptotic BH3-only protein BIM and repress both MYC and miR-17~92. These agents drive apoptosis and in vivo therapeutic effects in BCL-2–low MYC-driven lymphomas. In MYC-driven lymphomas where high BCL-2 expression is prevalent (eg, DEL and most DHL DLBCL), coadministration of an appropriate BH3 mimetic resensitizes these cells to therapy and enhances in vivo therapeutic effects via a BIM-dependent mechanism. These combination effects indicate the potential for a viable treatment option in resistant lymphoma.

## Acknowledgments

The authors acknowledge the patients who contributed samples used in this study. The authors also thank the Experimental Cancer

Medicine Centre–funded (C24563/A25171) University of Southampton, Faculty of Medicine Human Tissue Bank (Human Tissue Authority license 12009) for assistance with collecting and characterizing clinical material. Furthermore, the authors acknowledge the contribution of A. Steele for assistance with synergy calculations and Plexikon Inc. for provision of experimental compounds and guidance in their use. The authors also gratefully acknowledge the contribution of R. Fell and University Hospital Southampton Molecular Pathology department for undertaking cell line STR analysis. In addition, the authors thank A. Egle, L. Happe, E. Michalak, and A. Strasser for provision of BH3-only deficient E $\mu$ -myc LCLs.

This research was supported by a University of Southampton Faculty of Medicine Career Track Fellowship Award to M.J.C. Additional funding was provided by a Bloodwise Specialist Programme (15002) awarded to P.W.M.J., CRUK Centre funding (C328/A25139), and a CRUK Programme grant to G.P. (C2750/A23669).

## Authorship

Contribution: T.E.C.C. and M.J.C. performed experiments, analyzed results, and made the figures; M.S.C., P.W.M.J., and M.J.C. designed research; T.E.C.C., M.S.C. and M.J.C. wrote the manuscript with guidance and editing provided by G.P. and P.W.M.J.; Y.M. and B.P. provided biochemical data and identified PLX2853 and PLX51107; K.L.C., T.D.M., A.H.T., L.D., and V.L.E. assisted with in vivo experiments; and R.F. performed STR analysis of cell lines.

Conflict-of-interest disclosure: M.J.C. has, in the past, received funding from Gilead Sciences and Roche. M.S.C. is a retained consultant for Bioinvent and has performed educational and advisory roles for Boehringer Ingelheim, Merck KGaA, Baxalta, and GLG. He has received research funding from Bioinvent, Roche, Gilead, Iteos, UCB, and GSK. Y.M. and B.P. are employees of Plexikon Inc. The remaining authors declare no competing financial interests.

ORCID profiles: G.P., 0000-0002-9232-5691; P.W.M.J., 0000-0003-2306-4974; M.S.C., 0000-0003-2077-089X; M.J.C., 0000-0002-5198-5933.

Correspondence: Matthew J. Carter, Antibody and Vaccine Group, Centre for Cancer Immunology, Cancer Sciences Unit, Faculty of Medicine, University of Southampton, Southampton General Hospital, Tremona Rd, Southampton SO16 6YD, United Kingdom; e-mail: m.j.carter@soton.ac.uk.

## References

1. Martelli M, Ferreri AJ, Agostinelli C, Di Rocco A, Pfreundschuh M, Pileri SA. Diffuse large B-cell lymphoma. *Crit Rev Oncol Hematol*. 2013;87(2):146-171.
2. Dunleavy K. Double-hit lymphomas: current paradigms and novel treatment approaches. *Hematology Am Soc Hematol Educ Program*. 2014;2014:107-112.
3. Li S, Young KH, Medeiros LJ. Diffuse large B-cell lymphoma. *Pathology*. 2018;50(1):74-87.
4. Davies A, Cummin TE, Barrans S, et al. Gene-expression profiling of bortezomib added to standard chemioimmunotherapy for diffuse large B-cell lymphoma (REMoDL-B): an open-label, randomised, phase 3 trial. *Lancet Oncol*. 2019;20(5):649-662.
5. Dang CV. MYC on the path to cancer. *Cell*. 2012;149(1):22-35.

6. Delmore JE, Issa GC, Lemieux ME, et al. BET bromodomain inhibition as a therapeutic strategy to target c-Myc. *Cell*. 2011;146(6):904-917.
7. Fu LL, Tian M, Li X, et al. Inhibition of BET bromodomains as a therapeutic strategy for cancer drug discovery. *Oncotarget*. 2015;6(8):5501-5516.
8. Donati B, Lorenzini E, Ciarrocchi A. BRD4 and cancer: going beyond transcriptional regulation. *Mol Cancer*. 2018;17(1):164.
9. Hnisz D, Abraham BJ, Lee TI, et al. Super-enhancers in the control of cell identity and disease. *Cell*. 2013;155(4):934-947.
10. Lovén J, Hoke HA, Lin CY, et al. Selective inhibition of tumor oncogenes by disruption of super-enhancers. *Cell*. 2013;153(2):320-334.
11. Chapuy B, McKeown MR, Lin CY, et al. Discovery and characterization of super-enhancer-associated dependencies in diffuse large B cell lymphoma [published correction appears in *Cancer Cell*. 25(4):545]. *Cancer Cell*. 2013;24(6):777-790.
12. Green DR. The coming decade of cell death research: five riddles. *Cell*. 2019;177(5):1094-1107.
13. Llambi F, Moldoveanu T, Tait SW, et al. A unified model of mammalian BCL-2 protein family interactions at the mitochondria. *Mol Cell*. 2011;44(4):517-531.
14. Chen L, Willis SN, Wei A, et al. Differential targeting of prosurvival Bcl-2 proteins by their BH3-only ligands allows complementary apoptotic function. *Mol Cell*. 2005;17(3):393-403.
15. Xu Z, Sharp PP, Yao Y, et al. BET inhibition represses miR17-92 to drive BIM-initiated apoptosis of normal and transformed hematopoietic cells. *Leukemia*. 2016;30(7):1531-1541.
16. Baker EK, Taylor S, Gupte A, et al. BET inhibitors induce apoptosis through a MYC independent mechanism and synergise with CDK inhibitors to kill osteosarcoma cells. *Sci Rep*. 2015;5(1):10120.
17. Ennishi D, Mottok A, Ben-Neriah S, et al. Genetic profiling of MYC and BCL2 in diffuse large B-cell lymphoma determines cell of origin-specific clinical impact. *Blood*. 2017;129(20):2760-2770.
18. Thieblemont C, Stathis A, Inghirami G, et al. A phase 1 study of the BET-bromodomain inhibitor OTX015 in patients with non-leukemic hematologic malignancies. *Blood*. 2014;124(21):4417.
19. Blum K, Abramson J, Maris M, et al. 410 A phase I study of CPI-0610, a bromodomain and extra terminal protein (BET) inhibitor in patients with relapsed or refractory lymphoma. *Ann Oncol*. 2018;29(suppl 3):mdy048.
20. Amorim S, Stathis A, Gleeson M, et al. Bromodomain inhibitor OTX015 in patients with lymphoma or multiple myeloma: a dose-escalation, open-label, pharmacokinetic, phase 1 study. *Lancet Haematol*. 2016;3(4):e196-e204.
21. Dickinson M, Kamdar M, Huntly BJ, et al. A phase I study of molibresib (GSK525762), a selective bromodomain (BRD) and extra terminal protein (BET) inhibitor: results from part 1 of a phase I/II open label single agent study in subjects with non-Hodgkin's lymphoma (NHL) [abstract]. *Blood*. 2018; 132(suppl 1). Abstract 1682.
22. Piha-Paul SA, Sachdev JC, Barve M, et al. First-in-human study of mivebresib (ABBV-075), an oral pan-inhibitor of bromodomain and extra terminal proteins, in patients with relapsed/refractory solid tumors. *Clin Cancer Res*. 2019;25(21):6309-6319.
23. Ozer HG, El-Gamal D, Powell B, et al. BRD4 profiling identifies critical chronic lymphocytic leukemia oncogenic circuits and reveals sensitivity to PLX51107, a novel structurally distinct BET inhibitor. *Cancer Discov*. 2018;8(4):458-477.
24. Carter MJ, Cox KL, Blakemore SJ, et al. BCR-signaling-induced cell death demonstrates dependency on multiple BH3-only proteins in a murine model of B-cell lymphoma. *Cell Death Differ*. 2016;23(2):303-312.
25. Carter MJ, Cox KL, Blakemore SJ, et al. PI3K $\delta$  inhibition elicits anti-leukemic effects through Bim-dependent apoptosis. *Leukemia*. 2017;31(6):1423-1433.
26. Cragg MS, Howatt WJ, Bloodworth L, Anderson VA, Morgan BP, Glennie MJ. Complement mediated cell death is associated with DNA fragmentation. *Cell Death Differ*. 2000;7(1):48-58.
27. Adams JM, Harris AW, Pinkert CA, et al. The c-myc oncogene driven by immunoglobulin enhancers induces lymphoid malignancy in transgenic mice. *Nature*. 1985;318(6046):533-538.
28. Lin X, Huang X, Uziel T, et al. HEXIM1 as a robust pharmacodynamic marker for monitoring target engagement of BET family bromodomain inhibitors in tumors and surrogate tissues. *Mol Cancer Ther*. 2017;16(2):388-396.
29. Hogg SJ, Newbold A, Vervoort SJ, et al. BET inhibition induces apoptosis in aggressive B-cell lymphoma via epigenetic regulation of BCL-2 family members. *Mol Cancer Ther*. 2016;15(9):2030-2041.
30. Galluzzi L, Vitale I, Aaronson SA, et al. Molecular mechanisms of cell death: recommendations of the Nomenclature Committee on Cell Death 2018. *Cell Death Differ*. 2018;25(3):486-541.
31. Esteve-Arenys A, Valero JG, Chamorro-Jorganes A, et al. The BET bromodomain inhibitor CPI203 overcomes resistance to ABT-199 (venetoclax) by downregulation of BFL-1/A1 in vitro and in vivo models of MYC+/BCL2+ double hit lymphoma. *Oncogene*. 2018;37(14):1830-1844.
32. Li Y, Choi PS, Casey SC, Dill DL, Felsher DW. MYC through miR-17-92 suppresses specific target genes to maintain survival, autonomous proliferation, and a neoplastic state. *Cancer Cell*. 2014;26(2):262-272.
33. Fontana L, Fiori ME, Albin S, et al. Antagomir-17-5p abolishes the growth of therapy-resistant neuroblastoma through p21 and BIM. *PLoS One*. 2008; 3(5):e2236.
34. Koralov SB, Muljo SA, Galler GR, et al. Dicer ablation affects antibody diversity and cell survival in the B lymphocyte lineage. *Cell*. 2008;132(5):860-874.
35. Ventura A, Young AG, Winslow MM, et al. Targeted deletion reveals essential and overlapping functions of the miR-17 through 92 family of miRNA clusters. *Cell*. 2008;132(5):875-886.



36. Xiao C, Srinivasan L, Calado DP, et al. Lymphoproliferative disease and autoimmunity in mice with increased miR-17-92 expression in lymphocytes. *Nat Immunol*. 2008;9(4):405-414.
37. Egle A, Harris AW, Bouillet P, Cory S. Bim is a suppressor of Myc-induced mouse B cell leukemia. *Proc Natl Acad Sci USA*. 2004;101(16):6164-6169.
38. Haplo L, Cragg MS, Phipson B, et al. Maximal killing of lymphoma cells by DNA damage-inducing therapy requires not only the p53 targets Puma and Noxa, but also Bim. *Blood*. 2010;116(24):5256-5267.
39. Michalak EM, Jansen ES, Haplo L, et al. Puma and to a lesser extent Noxa are suppressors of Myc-induced lymphomagenesis. *Cell Death Differ*. 2009;16(5):684-696.
40. Lessene G, Czabotar PE, Sleebs BE, et al. Structure-guided design of a selective BCL-X(L) inhibitor. *Nat Chem Biol*. 2013;9(6):390-397.
41. Mason KD, Vandenberg CJ, Scott CL, et al. In vivo efficacy of the Bcl-2 antagonist ABT-737 against aggressive Myc-driven lymphomas. *Proc Natl Acad Sci USA*. 2008;105(46):17961-17966.
42. Souers AJ, Levenson JD, Boghaert ER, et al. ABT-199, a potent and selective BCL-2 inhibitor, achieves antitumor activity while sparing platelets. *Nat Med*. 2013;19(2):202-208.
43. Takimoto-Shimomura T, Tsukamoto T, Maegawa S, et al. Dual targeting of bromodomain-containing 4 by AZD5153 and BCL2 by AZD4320 against B-cell lymphomas concomitantly overexpressing c-MYC and BCL2. *Invest New Drugs*. 2019;37(2):210-222.
44. Johnson-Farley N, Veliz J, Bhagavathi S, Bertino JR. ABT-199, a BH3 mimetic that specifically targets Bcl-2, enhances the antitumor activity of chemotherapy, bortezomib and JQ1 in "double hit" lymphoma cells. *Leuk Lymphoma*. 2015;56(7):2146-2152.
45. Muthalagu N, Junttila MR, Wiese KE, et al. BIM is the primary mediator of MYC-induced apoptosis in multiple solid tissues. *Cell Rep*. 2014;8(5):1347-1353.
46. Bouillet P, Metcalf D, Huang DC, et al. Proapoptotic Bcl-2 relative Bim required for certain apoptotic responses, leukocyte homeostasis, and to preclude autoimmunity. *Science*. 1999;286(5445):1735-1738.
47. Enders A, Bouillet P, Puthalakath H, Xu Y, Tarlinton DM, Strasser A. Loss of the pro-apoptotic BH3-only Bcl-2 family member Bim inhibits BCR stimulation-induced apoptosis and deletion of autoreactive B cells. *J Exp Med*. 2003;198(7):1119-1126.
48. Chapuy B, Stewart C, Dunford A, et al. Molecular subtypes of diffuse large B cell lymphoma are associated with distinct pathogenic mechanisms and outcomes. *Nat Med*. 2018;24:679-690.
49. Tagawa H, Karube K, Tsuzuki S, Ohshima K, Seto M. Synergistic action of the microRNA-17 polycistron and Myc in aggressive cancer development. *Cancer Sci*. 2007;98(9):1482-1490.
50. Liu W, Ma Q, Wong K, et al. Brd4 and JMJD6-associated anti-pause enhancers in regulation of transcriptional pause release. *Cell*. 2013;155(7):1581-1595.
51. Frenzel A, Labi V, Chmielewski W, et al. Suppression of B-cell lymphomagenesis by the BH3-only proteins Bmf and Bad. *Blood*. 2010;115(5):995-1005.
52. Del Gaizo Moore V, Brown JR, Certo M, Love TM, Novina CD, Letai A. Chronic lymphocytic leukemia requires BCL2 to sequester prodeath BIM, explaining sensitivity to BCL2 antagonist ABT-737. *J Clin Invest*. 2007;117(1):112-121.
53. Fiskus W, Cai T, DiNardo CD, et al. Superior efficacy of cotreatment with BET protein inhibitor and BCL2 or MCL1 inhibitor against AML blast progenitor cells. *Blood Cancer J*. 2019;9(2):4.
54. Davis RE, Brown KD, Siebenlist U, Staudt LM. Constitutive nuclear factor kappaB activity is required for survival of activated B cell-like diffuse large B cell lymphoma cells. *J Exp Med*. 2001;194(12):1861-1874.
55. Ceribelli M, Kelly PN, Shaffer AL, et al. Blockade of oncogenic I $\kappa$ B kinase activity in diffuse large B-cell lymphoma by bromodomain and extraterminal domain protein inhibitors. *Proc Natl Acad Sci USA*. 2014;111(31):11365-11370.
56. Huang B, Yang X-D, Zhou M-M, Ozato K, Chen L-F. Brd4 coactivates transcriptional activation of NF-kappaB via specific binding to acetylated RelA. *Mol Cell Biol*. 2009;29(5):1375-1387.